Available online at www.sciencedirect.com

SCIENCE DIRECT

Developmental Biology 293 (2006) 461–472

DEVELOPMENTAL BIOLOGY

www.elsevier.com/locate/ydbio

Histone lysine trimethylation exhibits a distinct perinuclear distribution in Plzf-expressing spermatogonia

Christopher Payne, Robert E. Braun *

Department of Genome Sciences, University of Washington School of Medicine, Box 357730, 1705 N.E. Pacific Street, Seattle, WA 98195, USA

Received for publication 22 September 2005; revised 26 January 2006; accepted 13 February 2006
Available online 20 March 2006

Abstract

Chromatin structure plays an important role in the regulation of gene expression. Methylation of lysine residues on histone tails is an epigenetic mark that influences chromatin repression when specifically imparted on lysines 9 and 27 of histone H3, and on lysine 20 of H4. Histone lysines can be mono-, di-, and trimethylated, and all three modification states have been identified in different nuclear domains. Correlation of these methylated histone states to different stages of cell differentiation, however, is not extensive. Mammalian spermatogenesis is a developmental process ideal for studying the epigenetic control of differentiation. Maintenance of spermatogonial stem cells requires the transcriptional repressor Plzf, but a role for histone methylation has not been established. Here we show that Plzf-expressing spermatogonia completely lack monomethyl-H3-K27 and monomethyl-H4-K20, and contain very little monomethyl-H3-K9. Dimethylated H3-K27 and H4-K20 are detected as punctate foci in Plzf-positive cells, but dimethyl-H3-K9 is absent. Trimethylated H3-K9 and H4-K20 exhibit a unique perinuclear distribution that coincides with Plzf expression, localizing to punctate foci in more differentiated spermatogonia. Loss of Plzf correlates with increased punctate distribution of trimethylated H3-K9 and H4-K20 at the expense of perinuclear localization. These data signify the possible importance of different histone lysine methylation states in the epigenetic control of spermatogenesis.

Keywords: Histone modification; Germ cells; Spermatogonia; Epigenetics; Stem cells; Transcriptional repression

Introduction

Male germline stem cells are the undifferentiated cells within the mammalian testis that continually self-renew, while also differentiating to produce spermatozoa throughout sexual maturity of the animal. These cells comprise a sub-population of Type A spermatogonia and reside along the basal lamina of the germinal epithelium. One current model proposes that the A single (A_s) stem cells either renew themselves or divide into paired (A_{pr}) daughter cells that remain connected by an intercellular bridge (Huckins, 1971; Oakberg, 1971). A_{pr} spermatogonia divide further to form long chains of aligned (A_{al}) cells, which then generate the following progeny: the differentiating A_1–A_4, intermediate, and Type B spermatogonia; the pre-leptotene, leptotene, zygotene, and pachytene spermatocytes; the round and elongating spermatids; and ultimately the mature spermatozoa that form in the epididymis. A_s, A_{pr} and A_{al} spermatogonia express the transcriptional repressor Plzf (promyelocytic leukemia zinc-finger), recently shown to be required for the maintenance of germline stem cell self-renewal (Buaas et al., 2004; Costoya et al., 2004). Plzf is coexpressed with stem cell markers Oct 4 and GFRα-1 in A_s, A_{pr} and A_{al} spermatogonia (Buaas et al., 2004; unpublished observations), and loss-of-function mutations in Plzf result in germ cell depletion and sterility in adult male mice.

Initially identified as a chromosomal translocation partner with RARα in human patients with acute promyelocytic leukemia (Chen et al., 1993), Plzf is expressed in early hematopoietic progenitor cells and is downregulated during cell differentiation (Reid et al., 1995). Loss of Plzf results in anterior-to-posterior homeotic transformations in addition to the progressive loss of spermatogonia (Barna et al., 2000; Costoya et al., 2004), with alteration of HoxD gene expression affecting axial skeletal patterning. The BTB/POZ domain of Plzf recruits mammalian Polycomb group

* Corresponding author. Fax: +1 206 685 7301.
E-mail address: braun@u.washington.edu (R.E. Braun).

0012-1606/$ - see front matter © 2006 Elsevier Inc. All rights reserved.
doi:10.1016/j.ydbio.2006.02.013

Table 1
Distribution of methylated histones in germ cells of juvenile and adult mouse testes

	mono-Me Histones			di-Me Histones			tri-Me Histones		
	H3-K9	H3-K27	H4-K20	H3-K9	H3-K27	H4-K20	H3-K9	H3-K27	H4-K20
A_S, A_{pr}, A_{al} spermatogonia	+/− punc	−	−	−	+ punc, peri	+ punc	+ peri	+/− punc, peri	+ peri
A_1–A_4 spermatogonia	+/− punc	−	−	−	+ punc, peri	+ punc	+ punc, peri	+/− punc, peri	+/− punc, peri
In and Type B spermatogonia	+/− punc	+ diff	+ diff	+/− punc	+ punc, peri	+ punc	+ punc	+/− punc, peri	+ punc
spermatocytes:									
pre-Leptone	+	+	+	+	+	+	+	+/−	+
Leptotene	+	+	+	+	+	+	+	+/−	+
Zygotene	+	+	+	+	+	+	+	+/−	+
Pachytene	+/−	−	−	+	−	+	+[a]	−	+
Round spermatids	+/−	+	+	+/−	−	−	+	−	+
Elongating spermatids	−	+	+	−	−	−	+	−	+

+/− signifies weak staining; punc = punctate; peri = perinuclear; diff = diffuse.
[a] Present only in early Pachytene.

proteins like Bmi-1 to specific chromosomal regions, and associates with histone deacetylases at these sites (Reid et al., 1995; Barna et al., 2002). Bmi-1 is essential for adult hematopoietic and leukemic stem cell maintenance (Lessard and Sauvageau, 2003; Park et al., 2003), and fusion of the BTB/POZ domain of Plzf to RARα in humans with acute promyelocytic leukemia maintains undifferentiated myeloid cells through recruitment of co-repressors and histone deacetylases (Lin et al., 1998). Plzf thus influences the epigenetic state of these cells through repression of chromatin domains required for cell differentiation (Barna et al., 2002).

Post-translational modification of histone tails also regulates the epigenetic state of cells by influencing either transcriptional activation or gene silencing depending on the type of modification and the target residue (Lachner et al., 2003). Lysine acetylation and arginine methylation are broadly linked with transcriptional stimulation (Roth et al., 2001; Stallcup, 2001), while lysine methylation is known to influence both active and repressive chromatin structure in a context-specific manner (Lachner et al., 2003; Vakoc et al., 2005). Methylation of lysines 4, 36, and 79 on histone H3 associates with active genes, while methylation of lysines 9 and 27 on histone H3 and lysine 20 on histone H4 is linked to repressed domains. These modifications have been proposed to constitute a combinatorial 'histone code' that is then deciphered by nuclear proteins (Strahl and Allis, 2000; Jenuwein and Allis, 2001; Turner, 2002).

Lysine residues may be mono-, di-, and trimethylated, providing additional levels of complexity. Dimethyl-H3-K9 and trimethyl-H3-K27, for example, are epigenetic imprints found on the inactive X chromosome (Plath et al., 2003; Silva et al., 2003; Okamoto et al., 2004), while monomethyl-H3-K27, trimethyl-H3-K9, and trimethyl-H4-K20 are all associated with pericentric heterochromatin (Peters et al., 2003; Rice et al., 2003; Schotta et al., 2004). The three methylation states of H3-K9 were recently shown to exhibit differential subnuclear localization within cultured mammalian cell lines (Wu et al., 2005). It is not yet clear, however, whether these different methylation states also correspond to varying degrees of cell differentiation. It is possible that as cells become committed to specific lineages, they differentially express histone lysines in their mono-, di-, and trimethylated forms.

Using the mouse testis as a model for a comprehensive population of differentiating cells, we examined the distribution patterns of methylated histone lysines that correspond with transcriptional repression. Immunohistochemistry was performed with highly specific antibodies that recognize each of the different methylation states (mono-, di-, and tri-) for histone lysine residues H3-K9, H3-K27 and H4-K20 (Peters et al., 2003). Plzf was used as a marker for A_s, A_{pr} and A_{al} spermatogonia. Here, we identify a distinct perinuclear distribution of trimethyl-H3-K9 and trimethyl-H4-K20 in A_s, A_{pr} and A_{al} cells, with a shift toward punctate localization in *luxoid* mutants that lack functional Plzf. These results illustrate the importance of histone lysine methylation in the epigenetic control of germ cell self-renewal and differentiation.

Materials and methods

Mice

Wild type C57BL/6J and homozygous mutant C57BL/6.C3H/He *Plzf*^{lu} male mice were euthanized at either 1 week or 17 weeks of age for use

Fig. 1. Plzf-expressing spermatogonia lack monomethylated H3 lysine 27 and H4 lysine 20, and contain little monomethyl H3 lysine 9, in juvenile mouse testes. Immunofluorescence of mono-Me H3-K27 (green; A, A′), mono-Me H4-K20 (green; E, E′) and mono-Me H3-K9 (green; I, I′) in cross-sections of 1-week-old testes. Sections were co-stained with anti-Plzf antibody (red; B, B′, F, F′, J, J′) and DAPI (blue; C, C′, G, G′, K, K′), with color overlays depicted in panels D, D′, H, H′, L, L′. Staining areas outlined by dashed line boxes (A–L) are shown at higher magnification (A′–L′). Arrows panels in A′–L′ identify Plzf-positive spermatogonia. Asterisks in panels D and H indicate pachytene spermatocytes completely lacking mono-Me histone staining. Arrowheads in panels A′–L′ show nuclei with regions in which mono-Me histone staining does not coincide with DAPI foci.

in our experiments. All animals were housed in a barrier facility under normal light and dark conditions with free access to food and water. Generation of *luxoid* heterozygotes, $Plzf^{lu}$, has been described previously (Buaas et al., 2004). For the current experiments, male and female $Plzf^{+/lu}$ mice were intercrossed to generate $Plzf^{lu/lu}$ males. Genotyping was performed using genomic DNA isolated from mouse tails 5 days post partum by PCR

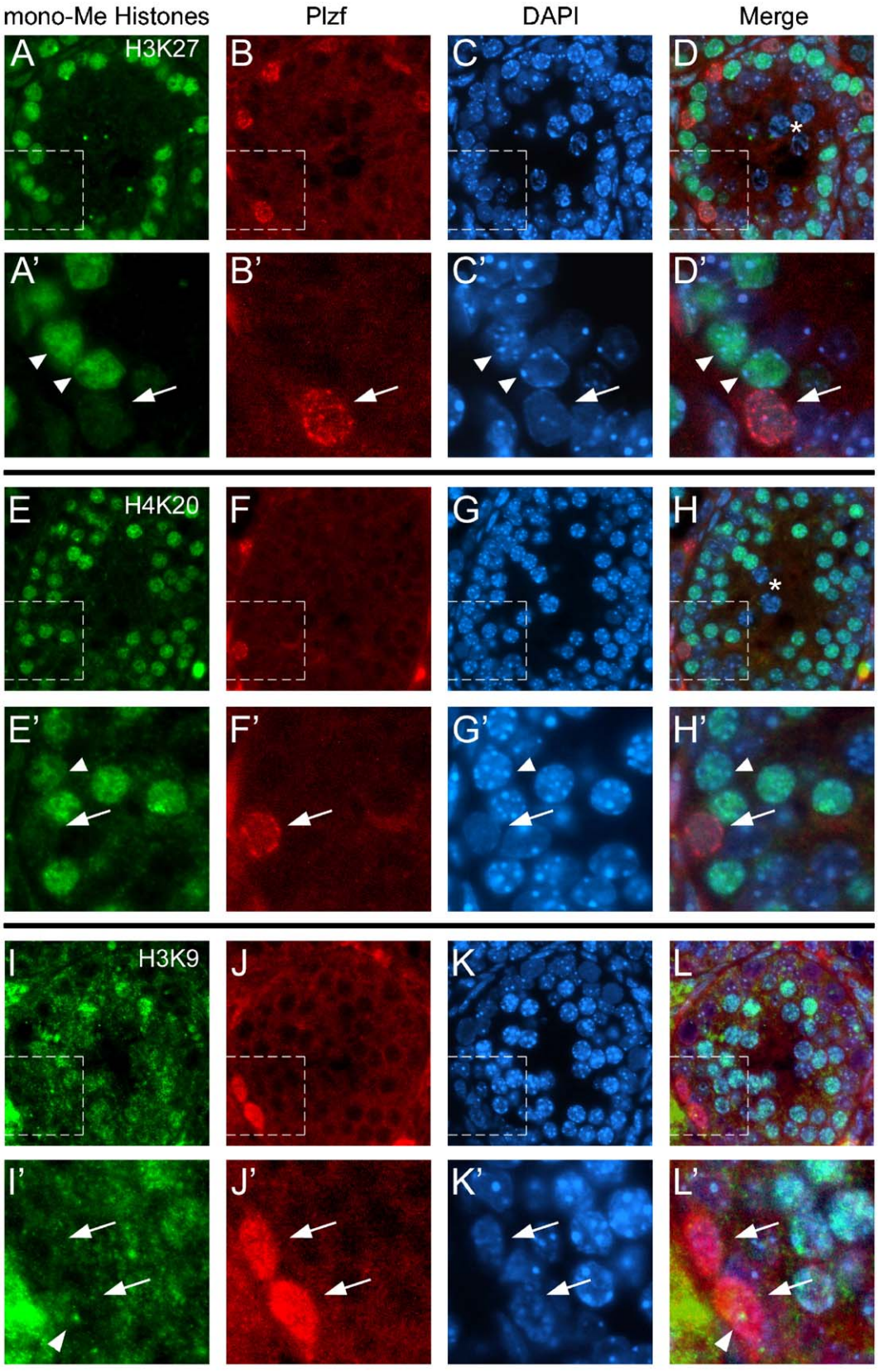

with the primer pair 5′-GTGCTAGCCTGCACCAGCTAGATGT-3′ and 5′-ACCGAGTAGATACCCAAATGCTTCTC-3′, followed by restriction enzyme digestion at 65°C withTsp45I to generate 481, 306 and 69 bp fragments specific to the *luxoid* mutant allele. The cycling profile used was 1 cycle of 5 min at 95°C, 35 cycles of 95°C for 30 s, 60°C for 30 s, 72°C for 1 min, and 1 cycle of 72°C for 7 min.

Histology and immunohistochemistry

Testes were fixed overnight at 4°C in Bouin's solution, rinsed in PBS, and embedded in paraffin. Five-micron sections were then cut, samples were deparaffinized and rehydrated, and antigen retrieval was performed by boiling the sections in 0.01 M citric acid in a microwave oven for 2 min at high power and 8 min at 50% power. Samples were rinsed in dH_20 and then blocked with 3% normal goat serum in PBS for 1 h at room temperature. Primary antibodies were diluted in PBS + 3% goat serum and added to the samples for overnight incubation at 4°C. Control reactions were performed by omitting primary antibodies from the incubations.

Following three rinses with PBS, samples were then incubated for 1 h in the dark at room temperature with fluorescence-conjugated secondary antibodies diluted in PBS + 3% goat serum. Three additional rinses with PBS were followed by the application of Vectashield anti-fade mounting medium (Vector Laboratories, Burlingame, CA) that contains the nuclear stain DAPI. Coverglass was mounted onto the microslides containing the testis sections and sealed with nail polish. Antibody staining was assessed using fluorescence microscopy at 400× and 600×.

Whole-mount immunocytochemistry was also performed on isolated seminiferous tubules. Five-millimeter length-wise sections of tubules were fixed overnight at 4°C with 4% paraformaldehyde in PBS, rinsed twice, and then taken step-wise through a dehydration/rehydration process using methanol. Following two additional rinses, samples were blocked with 3% normal goat serum in PBS for 1 h at room temperature, and immunostained using the protocol described above.

Antibodies

Rabbit polyclonal IgG antibodies raised against monomethyl-, dimethyl-, and trimethyl-H3-K9, H3-K27, and H4-K20 were generated and kindly provided by Antoine Peters (Friedrich Miescher Institute for Biomedical Research, Basel, Switzerland). All nine antibodies were used at a dilution of 1:1000. Mouse monoclonal anti-Plzf (Oncogene Research, now Calbiochem) and rabbit polyclonal anti-Plzf (Santa Cruz Biotechnology) were used 1:100, and the mouse monoclonal anti-c-Kit (PROGEN Biotechnik GmbH) was used 1:10. To detect the primary antibodies, AlexaFluor 488-anti-Rabbit and 568-anti-Mouse (Molecular Probes, Eugene, OR) were used 1:1000.

Scoring

Germ cell subtypes were identified using DAPI as a marker for heterochromatin and scoring parameters defined by Russell and colleagues (Chiarini-Garcia and Russell, 2001, 2002; Russell et al., 1990). In wild type juvenile and adult cross-sections, A_s, A_{pr} and A_{al} spermatogonia were collectively identified using Plzf as a marker (Buaas et al., 2004). Spermatogonial subtype A_1 exhibited no Plzf as well as very little DAPI staining along the nuclear envelope. Subtypes A_2, A_3, and A_4 exhibited DAPI staining along the envelope at approximate values of 10%, 25%, and 50%, respectively. Intermediate type spermatogonia contained even greater DAPI staining along the nuclear membrane, 75%–100%, with 1 or 2 compact nucleoli and larger DAPI-free regions (interchromosomal clear spaces) than those seen in A_4 cells. Type B spermatogonia exhibited intense foci of DAPI spaced periodically along the nuclear envelope, larger in appearance and frequency than those of the intermediate type. Pre-leptotene, leptotene, zygotene, and pachytene spermatocytes were identified by their location relative to the basal lamina in cross-sections of adult seminiferous tubules at defined epithelial stages, as well as by their distinctive DAPI patterns and the progressive increase in staining intensity (and decrease in DAPI-free regions). Type A spermatogonia were collectively identified by their characteristic DAPI staining and location along the basal lamina in $Plzf^{lu/lu}$ cross-sections.

Results

A_s, A_{pr} and A_{al} spermatogonia completely lack monomethylated H3-K27 and H4-K20, and contain little monomethyl-H3-K9

First, the distribution of monomethylated H3-K27 was analyzed. Examination of juvenile seminiferous tubule cross-sections revealed a complete absence of this epigenetic mark from all Type A spermatogonia, including Plzf-positive cells (Table 1; Figs. 1A–D′, arrow). Positive, diffuse staining was detected in the nuclei of intermediate and Type B spermatogonia, and characterization of adult cross-sections revealed monomethyl-H3-K27 distributing in pre-leptotene, leptotene, and zygotene spermatocytes (Table 1; Supplementary Figs. 1A–C, arrows). No staining was present in pachytene nuclei (Fig. 1D and Supplementary Figs. 1A–C, asterisks). In contrast to previous reports of selective enrichment at heterochromatic foci in ES cell nuclei (Peters et al., 2003), we observed these same monomethyl-H3-K27 antibodies to be excluded from the most intense DAPI-rich foci in nuclei positive for this epigenetic mark (Fig. 1D′, arrowheads). This distinct methylation pattern could be due to a difference in chromatin organization between spermatogonia and ES cells.

When monomethyl-H4-K20 was examined in both juveniles and adults, we observed a similar distribution and restriction to that of monomethyl-H3-K27. Specifically, it was absent from Type A spermatogonia that included Plzf-positive cells (Table 1; Figs. 1E–H′, arrow), as well as from pachytene spermatocytes (Table 1; Fig. 1H and Supplementary Figs. 1D–F, asterisks). It was present in both intermediate and Type B spermatogonia, and in spermatocytes at the pre-leptotene, leptotene, and zygotene stages (Table 1; Supplementary Figs. 1D–F, arrow). Most nuclei positive for monomethyl-H4-K20 distribution showed co-localization of the antibody with heterochromatin-rich regions, although some bright foci of DAPI lacked H4-K20 monomethylation (Fig. 1H′, arrowhead).

Assessment of monomethylated H3-K9 revealed positive staining in the nuclei of spermatocytes at all stages, as well as faint punctate foci observed in the nuclei of Type B,

Fig. 2. Plzf-expressing spermatogonia contain dimethylated H3 lysine 27 and H4 lysine 20, but not dimethyl H3 lysine 9, in juvenile mouse testes. Immunofluorescence of di-Me H3-K27 (green; A, A′), di-Me H4-K20 (green; E, E′) and di-Me H3-K9 (green; I, I′) in cross-sections of 1-week-old testes. Sections were co-stained with anti-Plzf antibody (red; B, B′, F, F′, J, J′) and DAPI (blue; C, C′, G, G′, K, K′), with color overlays depicted in panels D, D′, H, H′, L, L′. Staining areas outlined by dashed line boxes (A–L) are shown at higher magnification (A′–L′). Arrows in panels A′–L′ identify Plzf-positive spermatogonia. Asterisk in panel D indicates pachytene spermatocytes completely lacking di-Me histone staining. Arrowheads in panels A′–L′ show nuclei with regions in which di-Me histone staining does not coincide with DAPI foci.

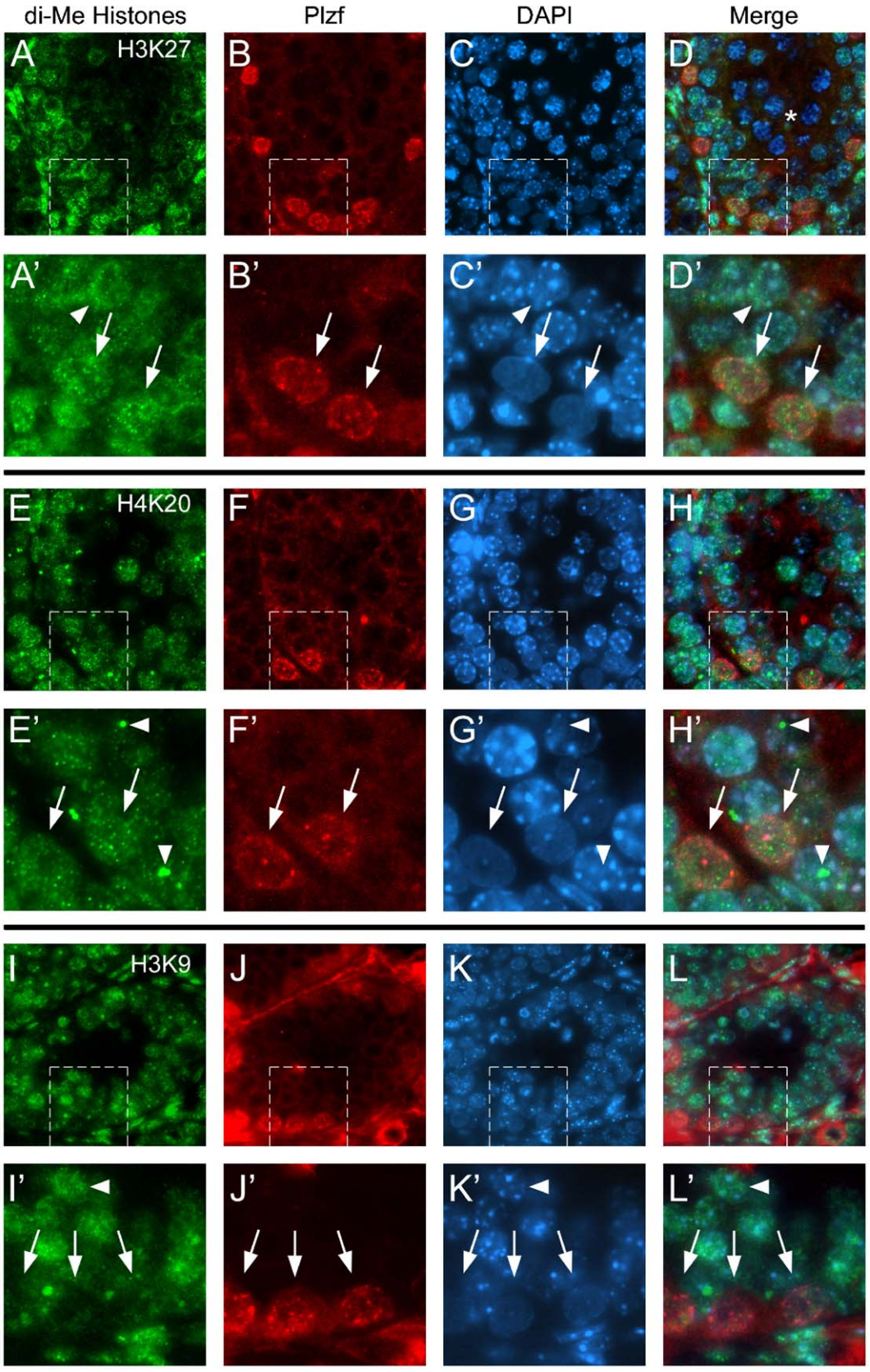
di-Me Histones
Plzf
DAPI
Merge
A
H3K27
B
C
D
*
A'
B'
C'
D'
E
H4K20
F
G
H
E'
F'
G'
H'
I
H3K9
J
K
L
I'
J'
K'
L'

intermediate, and Type A spermatogonia, including Plzf-positive cells (Table 1; Figs. 1I–L′, arrows). Very little monomethyl-H3-K9 was detected in Plzf-expressing spermatogonia, suggesting that its expression is limited to just a few 'spots' in A_s, A_{pr} and A_{al} cells (Fig. 1L′, arrowhead). Recent evidence demonstrates that H3-K9, in its monomethylated state, localizes to numerous foci within the nuclei of a variety of primary and immortalized cell types, but is excluded from DAPI-rich heterochromatin (Peters et al., 2003; Biron et al., 2004). We see a similar staining pattern here in this subset of male germ cells, with a punctate distribution that does not overlap with DAPI (Fig. 1L′, arrowhead).

Dimethylation of H3-K27 and H4-K20, but not H3-K9, occurs in A_s, A_{pr} and A_{al} spermatogonia

Next, we analyzed the staining pattern of dimethyl-H3-K27 in both juvenile and adult cross-sections. Punctate localization, along with weak perinuclear distribution, was observed in Type A, intermediate, and Type B spermatogonia (Table 1; Figs. 2A–D′). Faint punctate staining was also observed in pre-leptotene, leptotene, and zygotene spermatocytes, but was completely absent from pachytene nuclei (Table 1; Fig. 2D, asterisk). Minimal overlap of dimethyl-H3-K27 with heterochromatin-rich areas was detected, with some intense foci of antibody staining localized to regions free of DAPI (Fig. 2D′, arrowhead). Strikingly, similar patterns of H3-K27 dimethylation were observed in both Plzf-positive and Plzf-negative spermatogonia, raising the possibility that initial cell differentiation might precede any significant loss of dimethyl-H3-K27.

Examination of H4-K20 dimethylation in juveniles revealed a punctate distribution to numerous foci in the nuclei of all germ cells, from A_s, A_{pr} and A_{al} spermatogonia to pachytene spermatocytes (Table 1; Figs. 2E–H′). Assessment of adult cross-sections showed positive staining in pre-leptotene, leptotene, and zygotene spermatocytes as well, though this epigenetic mark was absent from round and elongating spermatids (Table 1). Like the nuclear distribution observed for dimethyl-H3-K27, minimal co-localization of H4-K20 dimethylation with heterochromatin was detected in cells, with numerous foci of antibody staining deficient in DAPI (Fig. 2H′, arrowheads).

When dimethylated H3-K9 was analyzed in both juveniles and adults, weak punctate staining was observed in the nuclei of both intermediate and Type B spermatogonia, with a more intense distribution in pre-leptotene, leptotene, zygotene, and pachytene spermatocytes (Table 1; Figs. 2I–L′). No dimethyl-H3-K9 was detected in Type A spermatogonia, including Plzf-positive cells (Figs. 2I′–L′, arrows). These staining patterns are consistent with recent findings of hyperdimethylation in the pericentromeric regions of autosomes, and at the X and Y chromosomes, in pachytene spermatocytes (Khalil et al., 2004). Yet, similar to the observations in early embryonic germ cells (Seki et al., 2005), some foci of dimethylated H3-K9 do not co-localize with DAPI-rich heterochromatin in these postnatal germ cells (Fig. 2L′, arrowhead).

Trimethylated H3-K9 and H4-K20, but not H3-K27, have an exclusively perinuclear distribution in A_s, A_{pr} and A_{al} spermatogonia

Characterization of trimethyl-H3-K9 revealed a striking perinuclear distribution in A_s, A_{pr} and A_{al} spermatogonia in juveniles (Figs. 3A–D′, arrow) and adults (Supplementary Figs. 2A–D′, arrow), with punctate localization in intermediate/Type B spermatogonia and spermatocytes through early pachytene stage, and a complete absence from late pachytene nuclei detected in adults (Table 1; Supplementary Figs. 1G–I and 2D′, asterisks). Trimethyl-H3-K9 was detected in early pachytene spermatocytes, but was greatly diminished by the mid-pachytene stage. A_1–A_4 spermatogonia exhibited both punctate and perinuclear staining in juveniles (Fig. 3D, asterisks). H3-K9 trimethylation showed extensive co-distribution with DAPI, suggesting its enrichment in heterochromatin (Fig. 3D′, arrowheads). The distinct trimethyl-H3-K9 staining patterns observed for the different types of spermatogonia raise the possibility that increasing cell differentiation may shift trimethyl-H3-K9 from a perinuclear to a punctate distribution.

When H4-K20 trimethylation was examined, a staining pattern similar to trimethyl-H3-K9 was observed. Trimethylated H4-K20 was perinuclear in A_s, A_{pr} and A_{al} spermatogonia in juveniles (Figs. 3I–L′, arrow) and adults (Supplementary Figs. 2I–L′, arrow), punctate in the nuclei of intermediate/Type B spermatogonia through pachytene spermatocytes, and both punctate and perinuclear in A_1–A_4 spermatogonia (Table 1). Unlike trimethyl-H3-K9, punctate H4-K20 trimethylation was also detected in late-stage pachytene nuclei. Consistent with recent reports that trimethyl-H4-K20 is a marker for constitutive heterochromatin (Kourmouli et al., 2004), extensive co-localization was observed between H4-K20 trimethylation and DAPI in those cells showing positive staining in juvenile cross-sections (Fig. 3L′, arrowhead). Thus, A_s, A_{pr} and A_{al} spermatogonia exhibit both trimethyl-H3-K9 and trimethyl-H4-K20 in an exclusively perinuclear pattern that is distinct from other germ cells.

Finally, we analyzed the distribution of trimethylated H3-K27. Very weak punctate and perinuclear localization was detected in germ cells at all stages from Type A spermatogonia through zygotene spermatocytes in juveniles (Figs. 3E–H′) and adults (Supplementary Figs. 2E–H′). Trimethyl-H3-K27 was absent from pachytene spermatocytes and both round and

Fig. 3. Plzf-expressing spermatogonia show exclusively perinuclear distribution of trimethylated H3 lysine 9 and H4 lysine 20, but not trimethyl H3 lysine 27, in juvenile mouse testes. Immunofluorescence of tri-Me H3-K9 (green; A, A′), tri-Me H3-K27 (green; E, E′) and tri-Me H4-K20 (green; I, I′) in cross-sections of 1-week-old testes. Sections were co-stained with anti-Plzf antibody (red; B, B′, F, F′, J, J′) and DAPI (blue; C, C′, G, G′, K, K′), with color overlays depicted panels in D, D′, H, H′, L, L′. Staining areas outlined by dashed line boxes (A–L) are shown at higher magnification (A′–L′). Arrows in panels A′–L′ identify Plzf-positive spermatogonia. Asterisks in panel D indicate A_1–A_4 spermatogonia. Arrowheads in panels A′–L′ show nuclei with regions in which tri-Me histone staining co-localizes with DAPI foci.

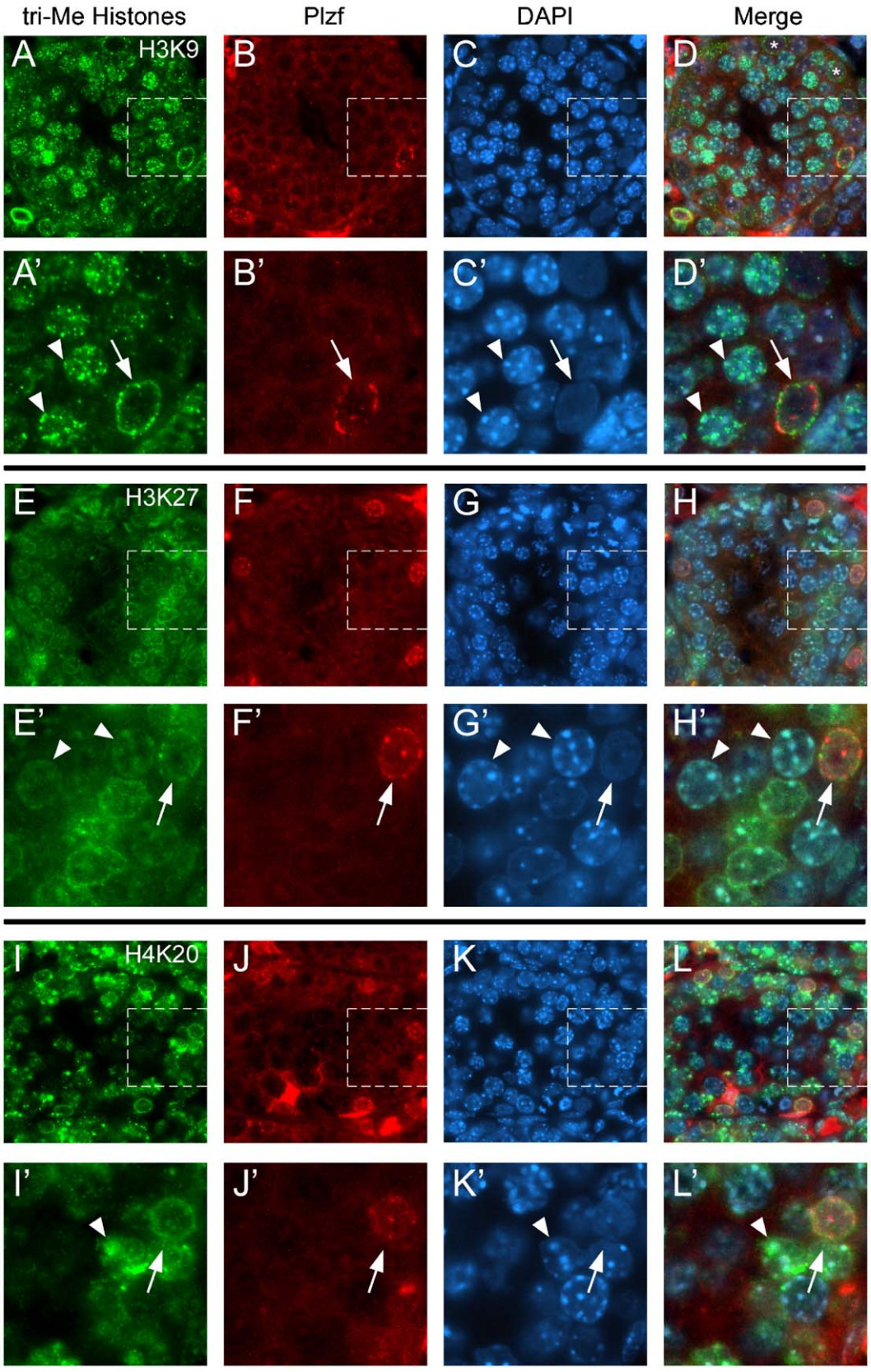
tri-Me Histones
Plzf
DAPI
Merge
A
H3K9
B
C
D
A'
B'
C'
D'
E
H3K27
F
G
H
E'
F'
G'
H'
I
H4K20
J
K
L
I'
J'
K'
L'

elongating spermatids (Table 1). Considerable co-localization between trimethyl-H3-K27 and DAPI was observed in spermatogonia and spermatocytes in juvenile cross-sections, although the relative staining intensity was weak (Fig. 3H′, arrowheads). These findings contrast with the intense H3-K27 trimethylation identified in the nuclei of migrating primordial germ cells of the mouse embryo (Seki et al., 2005).

In order to distinguish single A spermatogonia from pairs and chains, we examined seminiferous tubules processed by whole-mount immunocytochemistry. Fig. 4 verifies that trimethyl-H3-K9 distribution is perinuclear within A_s, A_{pr} and A_{al} spermatogonia, co-expressing with Plzf in these cells. Trimethyl-H4-K20 showed a similar pattern of expression (data not shown). We conclude that the distinctly perinuclear distribution of trimethylated H3-K9 and H4-K20 is coincident with Plzf expression.

Onset of c-Kit expression precedes monomethylated H3-K27 and H4-K20 detection, and coincides with perinuclear distribution of trimethylated H3-K9 and H4-K20

We next verified the absence of monomethylated H3-K27 and H4-K20 from Type A spermatogonia through co-immunostaining experiments with an antibody specific for the tyrosine kinase receptor c-Kit. Essential for maintaining primordial germ cells in the mouse embryo, and important for regulating spermatogenesis in the postnatal testis (reviewed by Rossi et al., 2000), c-Kit has been suggested to be a putative marker for the transition of A_{al} spermatogonia into A_1 (Schrans-Stassen et al., 1999). According to Schrans-Stassen et al., the c-Kit protein is first detected in postnatal male germ cells at the A_{al} stage and is observed in all subsequent spermatogonia and spermatocytes until the leptotene stage. Therefore, if monomethyl-H3-K27 and monomethyl-H4-K20 do not appear in the postnatal male germ cell lineage until the transition into intermediate spermatogonia, then a population of c-Kit-positive, monomethyl-histone-negative A_{al} and A_1–A_4 spermatogonia should be detected.

Examination of seminiferous tubule cross-sections showed that, indeed, some cells lying along the basal lamina completely lacked monomethyl-H3-K27 but were c-Kit-positive (Figs. 5A–D′, arrow), while others expressed both monomethyl-H3-K27 and c-Kit (Figs. 5A–D′, arrowhead). Similar results were obtained when cross-sections were examined for monomethyl-H4-K20 and c-Kit (data not shown). When c-Kit staining was then examined together with trimethyl-H3-K9 or trimethyl-H4-K20, some Type A spermatogonia exhibiting perinuclear distribution of the trimethylated histones were c-Kit-negative, while others were c-Kit positive (Figs. 5E–H′, arrows; data shown for trimethyl-H4-K20). These results suggest that the perinuclear distribution of trimethylated histone lysines coincides with the expression of c-Kit in a subset of Type A spermatogonia, presumably A_{al}. For both sets of experiments, the use of c-Kit identifies key spatio-temporal transition periods: the onset of monomethylated H3-K27 and H4-K20, and the redistribution of trimethylated H3-K9 and H4-K20.

Loss of Plzf results in increased punctate distribution of trimethyl-H3-K9 and trimethyl-H4-K20 in Type A spermatogonia

To test whether Plzf plays a role in regulating the spatial distribution of trimethyl-H3-K9 and H4-K20 in the nuclei of Type A spermatogonia, we examined the staining patterns of these histone lysine trimethylation states in the testes of *luxoid* mutant mice. The *luxoid* mutant contains a nonsense mutation in the gene encoding Plzf and results in a severely truncated Plzf protein lacking all of its DNA-binding zinc finger domains (Buaas et al., 2004). $Plzf^{lu/lu}$ males progressively lose their germline stem cells and become sterile, with many of their seminiferous tubules rendered agametic. Examination of $Plzf^{lu/lu}$ testis cross-sections revealed that in those seminiferous tubules that still contained germ cells, both trimethyl-H3-K9 and trimethyl-H4-K20 showed increased punctate distribution in the nuclei of Type A spermatogonia when compared to wild type (Figs. 6A–H′ and Supplementary Figs. 3A–H′, arrows). Some perinuclear staining could still be seen in these $Plzf^{lu/lu}$ cells, but was accompanied by numerous large foci not detected in the nuclei of corresponding wild type cells. No $Plzf^{lu/lu}$ Type A spermatogonia examined had exclusively perinuclear trimethyl-H3-K9 or trimethyl-H4-K20, despite containing DAPI staining patterns that were characteristic of A_s, A_{pr} and A_{al} spermatogonia. Comparison of $Plzf^{lu/lu}$ testes isolated at 1 week and at 17 weeks of age showed little difference in

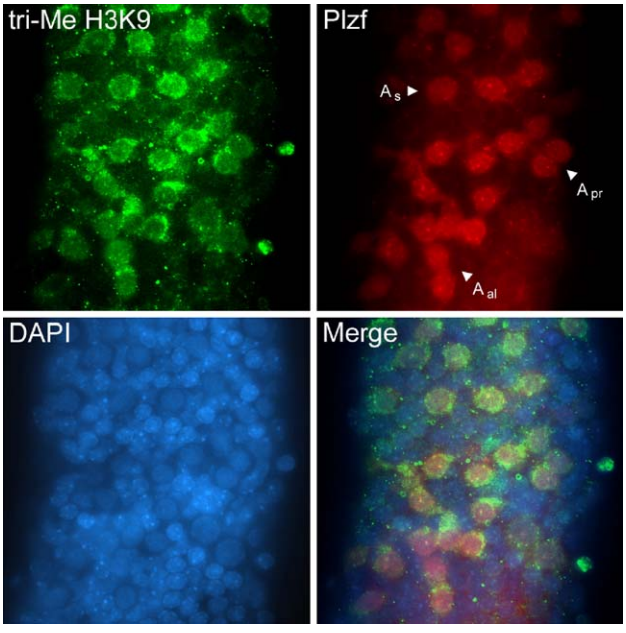

Fig. 4. Co-immunofluorescence localization of trimethyl H3-K9 and Plzf in A_s, A_{pr} and A_{al} spermatogonia. Immunofluorescence of tri-Me H3-K9 (green), Plzf (red) and DAPI (blue), with color overlay (merge), in whole-mount seminiferous tubules isolated from 1-week-old testes. Arrowheads indicate single (A_s), paired (A_{pr}) and aligned (A_{al}) Type A spermatogonia that are Plzf-positive.

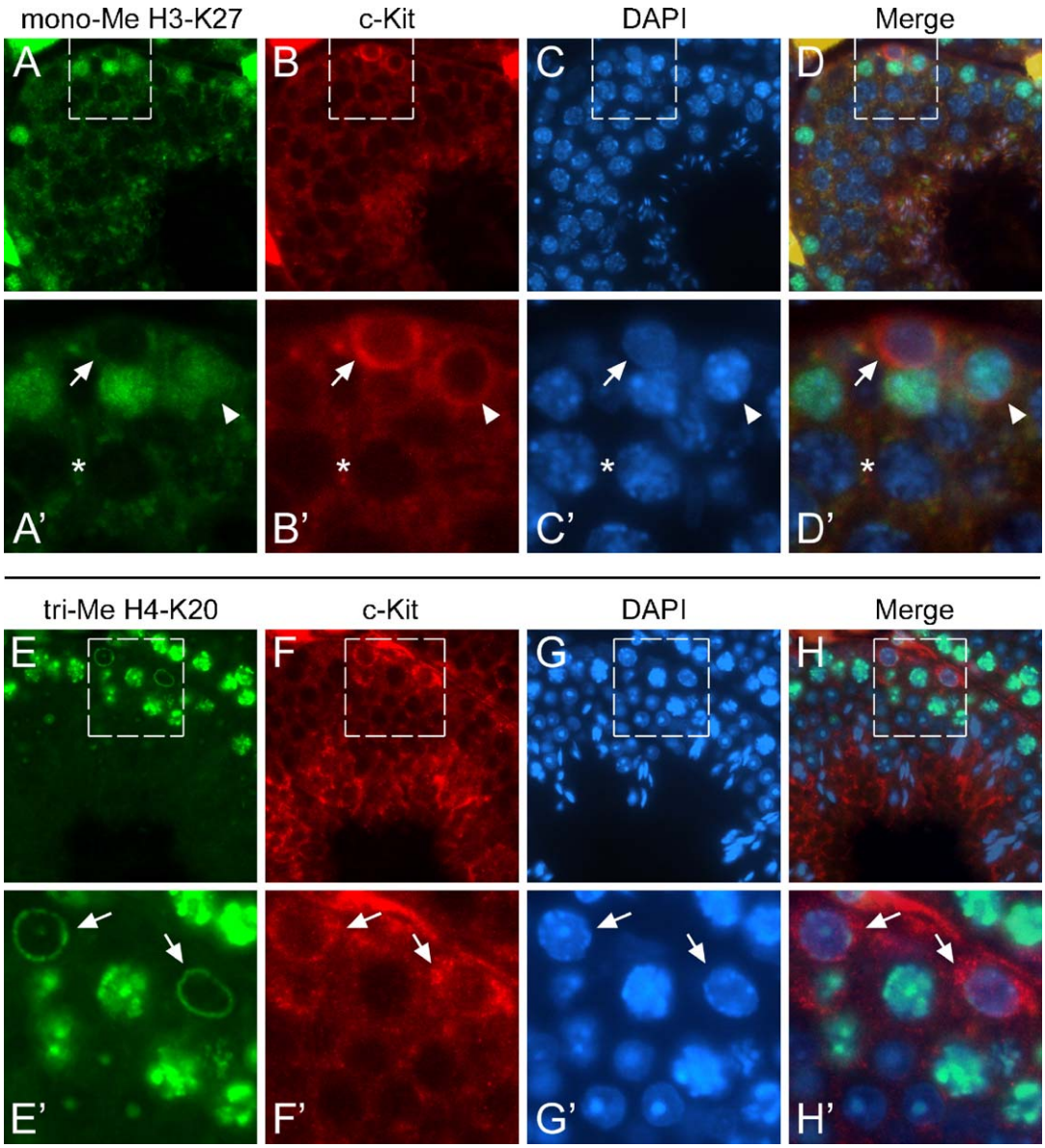

Fig. 5. c-Kit coincides with the perinuclear distribution of trimethyl-H4-K20, and precedes the expression of monomethyl-H3-K27. Immunofluorescence of mono-Me H3-K27 (green; A, A′) and tri-Me H4-K20 (green; E, E′) in cross-sections of 17-week-old testes. Sections were co-stained with anti-c-Kit antibody (red; B, B′, F, F′) and DAPI (blue; C, C′, G, G′), with color overlays depicted panels in D, D′, H, H′. Staining areas outlined by dashed line boxes (A–H) are shown at higher magnification (A′–H′). Arrows in panels A′–H′ identify c-Kit-positive cells. Arrowhead in panels A′–D′ shows c-Kit positive cell that is also faintly positive for mono-Me H3-K27. Asterisks in panels A′–D′ indicate pachytene spermatocytes completely lacking mono-Me histone staining.

histone trimethyl-lysine staining patterns within the nuclei of the remaining Type A spermatogonia.

Discussion

We have shown that the repressive histone methylation states of H3-K9, H3-K27 and H4-K20 are present within the nuclei of postnatal male germ cells, and that they distribute predominantly as punctate foci in differentiated spermatogonia and spermatocytes. The trimethylated states of H3-K9 and H4-K20 show particular enrichment in A_s, A_{pr} and A_{al} spermatogonia and display an exclusively perinuclear distribution not observed in other germ cell types. Both of these trimethylated states are known to occupy domains in pericentromeric heterochromatin (Peters et al., 2003; Rice et al., 2003), and are considered to have significant influence on chromatin structure and function, imparting an epigenetic silencing more-lasting than either of the mono- or dimethyl states (Biron et al., 2004). The lack of monomethyl-H3-K27 and H4-K20 in Plzf-expressing cells suggests that A_s, A_{pr} and A_{al} spermatogonia preferentially contain these histone lysine residues in their di- and trimethylated states, which in turn could reflect a higher degree of chromatin silencing to keep these cells less differentiated.

In contrast to the perinuclear H3-K9 trimethylation we observed in A_s, A_{pr} and A_{al} spermatogonia, other studies using cultured cell lines report trimethyl-H3-K9 distributing to clusters of intranuclear foci, with dimethyl-H3-K9 instead localizing at the nuclear periphery (Wu et al., 2005). In those

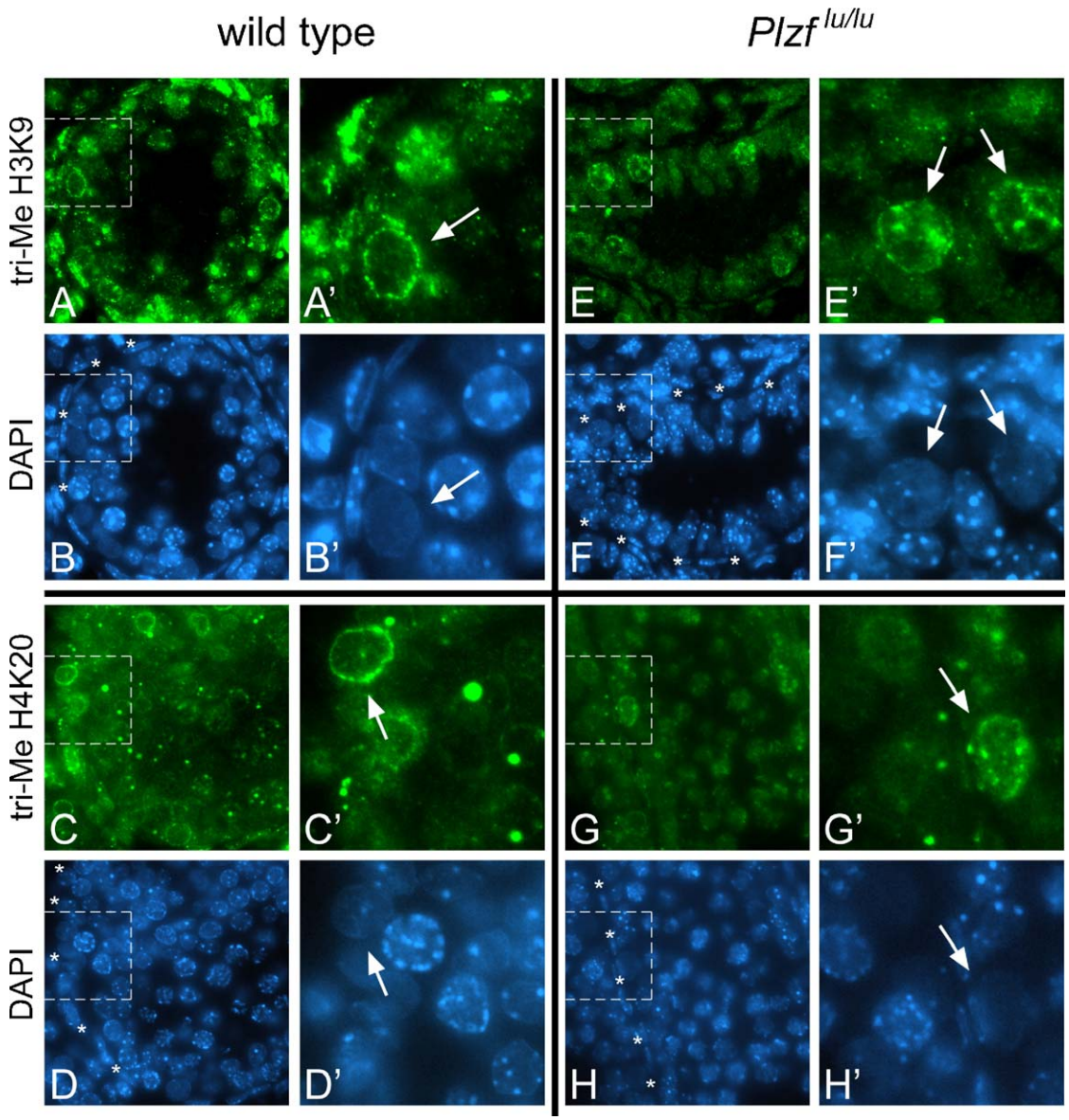

Fig. 6. Altered distribution of trimethylated H3-K9 and H4-K20 in juvenile testes of *Plzf*$^{lu/lu}$ mice. Immunofluorescence of tri-Me H3-K9 (green: A, A′, E, E′), and tri-Me H4-K20 (green: C, C′, G, G′) in cross-sections of 1-week-old testes isolated from wild type (A–D′) and *Plzf*$^{lu/lu}$ (E–H′) mice. Sections were co-stained with DAPI (blue; B, B′, D, D′, F, F′, H, H′). Staining areas outlined by dashed line boxes (A–H) are shown at higher magnification (A′–H′). Arrows in panels A′–H′ identify Type A spermatogonia. Asterisks in B, D, F, H indicate the location of the basal lamina in the seminiferous tubules.

studies trimethyl-H3-K9, unlike the dimethylated form, does not exhibit perinuclear distribution in C127, CHO, or HeLa cells. The distinct H3-K9 distribution patterns exhibited here by male germ cells suggest that the epigenetic marks of histone lysine methylation may be cell lineage-specific.

Absence of mono-, di-, and trimethylated H3-K27 from pachytene spermatocytes appears significant. Histone methylation was, until recently, considered an irreversible process. Identification of the LSD1 demethylase, however, has demonstrated that both mono- and dimethyl-H3K4, as well as mono- and dimethyl-H3-K9 could be demethylated through an amine oxidase reaction (Shi et al., 2004; Metzger et al., 2005). Our finding that monomethyl-H4-K20, trimethyl-H3-K9, and all three states (mono-, di-, and tri-) of methylated H3-K27 are absent from pachytene spermatocytes (late-stage pachytene in the case of trimethyl-H3-K9) raises the possibility that histone demethylation might occur just prior to meiotic division. Further studies are warranted to determine whether absence of these epigenetic marks is due to active demethylation or simply due to turnover of methylated lysines.

The perinuclear distribution of trimethyl-H3-K9 and trimethyl-H4-K20 could be indicative of heterochromatin lining the nuclear envelope. Numerous studies using both light and transmission electron microscopy have interpreted A_s, A_{pr} and A_{al} spermatogonia as having little to no heterochromatin along the nuclear periphery (Buaas et al., 2004; Chiarini-Garcia and Russell, 2001, 2002; Russell et al., 1990). This interpretation has contributed to the classical scoring system used to assess the different stages of male germ cells. Other reports, however, have shown appreciable levels of heterochromatin bound to the

nuclear membrane in cells positive for GFRα-1, a receptor restricted to A_s, A_{pr} and A_{al} spermatogonia within the testis (Dettin et al., 2003). The nuclear stain DAPI, which preferentially intercalates pericentric heterochromatin, shows faint perinuclear distribution in cells positive for Plzf (Buaas et al., 2004). Trimethyl-H3-K9 and trimethyl-H4-K20, markers for constitutive heterochromatin in a variety of cells, exhibit significant perinuclear localization exclusively in Plzf-positive spermatogonia. Taken together, we conclude that A_s, A_{pr} and A_{al} spermatogonia are likely to contain the majority of what little heterochromatin they have along the nuclear envelope, and that the perinuclear distribution of trimethyl-H3-K9 and trimethyl-H4-K20 could be a novel marker for male germline stem cells.

Most striking is the absence of perinuclear H3-K9 and H4-K20 trimethylation in intermediate and Type B spermatogonia, and the presence of both punctate and perinuclear distribution in A_1–A_4 cells. This suggests that a shift in distribution to punctate foci might correlate with increasing cell differentiation. Plzf expression is not detected in A_1–A_4, intermediate, or Type B spermatogonia, raising the possibility that Plzf might play a role in maintaining an exclusively perinuclear organization of heterochromatin. Examination of histone lysine trimethylation in Type A spermatogonia lacking Plzf indeed shows a relative increase in punctate foci throughout the nuclei. We conclude from these data that a loss of Plzf results in increased punctate distribution of trimethyl-H3-K9 and trimethyl-H4-K20 in Type A spermatogonia at the expense of perinuclear localization. These results identify a novel role for Plzf in maintenance of the spatial distribution of trimethylated histones corresponding to chromatin repression in undifferentiated cells. H3-K9 and H4-K20 trimethylation is also shown, for the first time, to exhibit unique subnuclear expression patterns that could influence the epigenetic states of A_s, A_{pr} and A_{al} spermatogonia and male germline stem cell self-renewal.

Acknowledgments

We are grateful to members of the Braun Laboratory for helpful comments and discussions during the preparation of the manuscript. This work was supported by a grant to R.E.B. from the NICHD/NIH Contraceptive Development Research Centers Program (U54 HD4254). C.P. received support as a research fellow from the NICHD/NIH Training in Reproductive Biology Grant (5T32 H007453).

Appendix A. Supplementary data

Supplementary data associated with this article can be found in the online version at doi:10.1016/j.ydbio.2006.02.013.

References

Barna, M., Hawe, N., Niswander, L., Pandolfi, P.P., 2000. Plzf regulates limb and axial skeletal patterning. Nat. Genet. 25, 166–172.

Barna, M., Merghoub, T., Costoya, J.A., Ruggero, D., Branford, M., Bergia, A., Samori, B., Pandolfi, P.P., 2002. Plzf mediates transcriptional repression of HoxD gene expression through chromatin remodeling. Dev. Cell 3, 499–510.

Biron, V.L., McManus, K.J., Hu, N., Hendzel, M.J., Underhill, D.A., 2004. Distinct dynamics and distribution of histone methyl-lysine derivatives in mouse development. Dev. Biol. 276, 337–351.

Buaas, F.W., Kirsh, A.L., Sharma, M., McLean, D.J., Morris, J.L., Griswold, M.D., de Rooij, D.G., Braun, R.E., 2004. Plzf is required in adult male germ cells for stem cell self-renewal. Nat. Genet. 36, 647–652.

Chen, Z., Brand, N.J., Chen, A., Chen, S.J., Tong, J.H., Wang, Z.Y., Waxman, S., Zelent, A., 1993. Fusion between a novel Kruppel-like zinc finger gene and the retinoic acid receptor-alpha locus due to a variant t(11;17) translocation associated with acute promyelocytic leukaemia. EMBO J. 12, 1161–1167.

Chiarini-Garcia, H., Russell, L.D., 2001. High-resolution light microscopic characterization of mouse spermatogonia. Biol. Reprod. 65, 1170–1178.

Chiarini-Garcia, H., Russell, L.D., 2002. Characterization of mouse spermatogonia by transmission electron microscopy. Reproduction 123, 567–577.

Costoya, J.A., Hobbs, R.M., Barna, M., Cattoretti, G., Manova, K., Sukhwani, M., Orwig, K.E., Wolgemuth, D.J., Pandolfi, P.P., 2004. Essential role of Plzf in maintenance of spermatogonial stem cells. Nat. Genet. 36, 653–659.

Dettin, L., Ravindranath, N., Hofmann, M.C., Dym, M., 2003. Morphological characterization of the spermatogonial subtypes in the neonatal mouse testis. Biol. Reprod. 69, 1565–1571.

Huckins, C., 1971. The spermatogonial stem cell population in adult rats: I. Their morphology, proliferation and maturation. Anat. Rec. 169, 533–557.

Jenuwein, T., Allis, C.D., 2001. Translating the histone code. Science 293, 1074–1080.

Khalil, A.M., Boyar, F.Z., Driscoll, D.J., 2004. Dynamic histone modifications mark sex chromosome inactivation and reactivation during mammalian spermatogenesis. Proc. Natl. Acad. Sci. U.S.A. 101, 16583–16587.

Kourmouli, N., Jeppesen, P., Mahadevhaiah, S., Burgoyne, P., Wu, R., Gilbert, D.M., Bongiorni, S., Prantera, G., Fanti, L., Pimpinelli, S., Shi, W., Fundele, R., Singh, P.B., 2004. Heterochromatin and tri-methylated lysine 20 of histone H4 in animals. J. Cell Sci. 117, 2491–2501.

Lachner, M., O'Sullivan, R.J., Jenuwein, T., 2003. An epigenetic road map for histone lysine methylation. J. Cell Sci. 116, 2117–2124.

Lessard, J., Sauvageau, G., 2003. Bmi-1 determines the proliferative capacity of normal and leukaemic stem cells. Nature 423, 255–260.

Lin, R.J., Nagy, L., Inoue, S., Shao, W., Miller Jr., W.H., Evans, R.M., 1998. Role of the histone deacetylase complex in acute promyelocytic leukaemia. Nature 391, 811–814.

Metzger, E., Wissmann, M., Yin, N., Müller, J.M., Schneider, R., Peters, A.H.F. M., Günther, T., Buettner, R., Schüle, R., 2005. LSD1 demethylates repressive histone marks to promote androgen-receptor-dependent transcription. Nature 437 (7057), 436–439.

Oakberg, E., 1971. Spermatogonial stem-cell renewal in the mouse. Anat. Rec. 169, 515–531.

Okamoto, I., Otte, A.P., Allis, C.D., Reinberg, D., Heard, E., 2004. Epigenetic dynamics of imprinted X inactivation during early mouse development. Science 303, 644–649.

Park, I.K., Qian, D., Kiel, M., Becker, M.W., Pihalja, M., Weissman, I.L., Morrison, S.J., Clarke, M.F., 2003. Bmi-1 is required for maintenance of adult self-renewing haematopoietic stem cells. Nature 423, 302–305.

Peters, A.H., Kubicek, S., Mechtler, K., O'Sullivan, R.J., Derijck, A.A., Perez-Burgos, L., Kohlmaier, A., Opravil, S., Tachibana, M., Shinkai, Y., Martens, J.H., Jenuwein, T., 2003. Partitioning and plasticity of repressive histone methylation states in mammalian chromatin. Mol. Cell 12, 1577–1589.

Plath, K., Fang, J., Mlynarczyk-Evans, S.K., Cao, R., Worringer, K.A., Wang, H., de la Cruz, C.C., Otte, A.P., Panning, B., Zhang, Y., 2003. Role of histone H3 lysine 27 methylation in X inactivation. Science 300, 131–135.

Reid, A., Gould, A., Brand, N., Cook, M., Strutt, P., Li, J., Licht, J., Waxman, S., Krumlauf, R., Zelent, A., 1995. Leukemia translocation gene, PLZF, is expressed with a speckled nuclear pattern in early hematopoietic progenitors. Blood 86, 4544–4552.

Rice, J.C., Briggs, S.D., Ueberheide, B., Barber, C.M., Shabanowitz, J., Hunt, D.F., Shinkai, Y., Allis, C.D., 2003. Histone methyltransferases direct different degrees of methylation to define distinct chromatin domains. Mol. Cell 12, 1591–1598.

Rossi, P., Sette, C., Dolci, S., Geremia, R., 2000. Role of c-kit in mammalian spermatogenesis. J. Endocrinol. Invest. 23, 609–615.

Roth, S.Y., Denu, J.M., Allis, C.D., 2001. Histone acetyltransferases. Annu. Rev. Biochem. 70, 81–120.

Russell, L.D., Ettlin, R.A., Sinha Hikim, A.P., Clegg, E.D., 1990. Histological and Histopathological Evaluation of the Testis. Cache River Press, USA.

Schotta, G., Lachner, M., Sarma, K., Ebert, A., Sengupta, R., Reuter, G., Reinberg, D., Jenuwein, T., 2004. A silencing pathway to induce H3-K9 and H4-K20 trimethylation at constitutive heterochromatin. Genes Dev. 18, 1251–1262.

Schrans-Stassen, B.H.G.J., Van De Kant, H.J.G., De Rooij, D.G., Van Pelt, A.M.M., 1999. Differential expression of c-kit in mouse undifferentiated and differentiating type A spermatogonia. Endocrinology 140, 5894–5900.

Seki, Y., Hayashi, K., Itoh, K., Mizugaki, M., Saitou, M., Matsui, Y., 2005. Extensive and orderly reprogramming of genome-wide chromatin modifications associated with specification and early development of germ cells in mice. Dev. Biol. 278, 440–458.

Shi, Y., Lan, F., Matson, C., Mulligan, P., Whetstine, J.R., Cole, P.A., Casero, R.A., Shi, Y., 2004. Histone demethylation mediated by the nuclear amine oxidase homolog LSD1. Cell 119, 941–953.

Silva, J., Mak, W., Zvetkova, I., Appanah, R., Nesterova, T.B., Webster, Z., Peters, A.H., Jenuwein, T., Otte, A.P., Brockdorff, N., 2003. Establishment of histone H3 methylation on the inactive X chromosome requires transient recruitment of Eed–Enx1 polycomb group complexes. Dev. Cell 4, 481–495.

Stallcup, M.R., 2001. Role of protein methylation in chromatin remodeling and transcriptional regulation. Oncogene 20, 3014–3020.

Strahl, B.D., Allis, C.D., 2000. The language of covalent histone modifications. Nature 403, 41–45.

Turner, B.M., 2002. Cellular memory and the histone code. Cell 111, 285–291.

Vakoc, C.R., Mandat, S.A., Olenchock, B.A., Blobel, G.A., 2005. Histone H3 lysine 9 methylation and HP1γ are associated with transcription elongation through mammalian chromatin. Mol. Cell 19, 381–391.

Wu, R., Terry, A.V., Singh, P.B., Gilbert, D.M., 2005. Differential subnuclear localization and replication timing of histone H3 lysine 9 methylation states. Mol. Biol. Cell 16, 2872–2881.